

Non-mesonic Weak Decays of Light Hypernuclei in the Direct Quark and the One-Pion Exchange Mechanisms

T. Inoue^{(a)*}, M. Oka^(b), T. Motoba^(c) and K. Itonaga^(d)

^(a) *Department of Physics, University of Tokyo, Bunkyo, Tokyo 112 Japan*

^(b) *Department of Physics, Tokyo Institute of Technology, Meguro, Tokyo 152 Japan*

^(c) *Laboratory of Physics, Osaka Electro-Communication University,
Neyagawa, Osaka 572 Japan*

^(d) *Laboratory of Physics, Miyazaki Medical College, Miyazaki 889-16 Japan*

Contributions of the direct quark mechanism are studied in the nonmesonic weak decays of light hypernuclei. The $\Lambda N \rightarrow NN$ transition is described by the one pion exchange mechanism and the direct quark mechanism, induced by the four-quark vertices in the effective weak Hamiltonian. By employing a realistic wave function of the Λ inside the hypernuclei, nonmesonic decay rates of ${}^4_{\Lambda}\text{H}$, ${}^4_{\Lambda}\text{He}$, and ${}^5_{\Lambda}\text{He}$ are calculated. The results show that the direct quark mechanism is significantly large and gives a large $\Delta I = 3/2$ contribution in the $J = 0$ channel. The relative phase between the one-pion exchange and the direct-quark contributions is determined so that the effective weak Hamiltonian for quarks give both of them consistently. We find that the sum of these two contributions reproduce the current available experimental data fairly well.

*e-mail: inoue@nt.phys.s.u-tokyo.ac.jp

1. Introduction

An $S = -1$ hypernucleus decays from its ground state to non-strange hadrons, emitting roughly 170 MeV ($\sim M_\Lambda - M_N$) of extra energy[1]. As is the decay of free Λ , it can emit a pion + 30 MeV. It is, however, known that the pionic decay is strongly suppressed because the remaining energy is too small for the produced nucleon to go above the Fermi surface of the nucleus. Consequently, the main decay mode of (heavy) hypernuclei is the decay without a pion emission, called nonmesonic decay. The nonmesonic decay releases the full 170 MeV of energy and therefore is not Pauli blocked. The final state is dominated by two nucleons ejected in the opposite directions so that the momentum is conserved, although three-body processes may not be negligible[2]. A natural way of describing the nonmesonic decay is to assume that the emitted (virtual) pion from the Λ decay is absorbed by a nucleon in the nucleus. This is called the one-pion exchange (OPE) weak transition and has been studied by many authors[3,4,5,6,7,8].

On the other hand, the final NN state has a large relative momentum so that the short-range interactions are also important[9,10]. Two of the present authors have proposed that the quark structure of the baryons provides a new mechanism for the nonmesonic $\Lambda N \rightarrow NN$, called direct quark (DQ) mechanism[11,12,13,14]. We calculated transition amplitudes for the S wave initial states in both OPE and DQ, and found that the contribution of the DQ is in general as large as that of the OPE. DQ is even dominant in the $L = 0$ to $L = 0$ transitions. It gives a large contribution in the $J=0$ ($L=0, S=0$) transitions and thus contributes to the nn ($I=1$) final state. We found that the nn/pn ratio of the final state becomes larger than that predicted in OPE. It was also found that the $J = 0$ transition amplitudes have a significant $\Delta I = 3/2$ contribution.

In this paper, we apply the DQ transition potential to the decay of three light hypernuclei, ${}^4_\Lambda\text{H}$, ${}^4_\Lambda\text{He}$, and ${}^5_\Lambda\text{He}$ in order to study how the features of DQ are reflected in the decay observables of simple hypernuclei. We employ realistic wave functions for the hypernuclei, and evaluate the matrix elements of the two-body weak transition potentials in OPE and DQ, and also of the potential given by the superposition of OPE and DQ. The relative phase of OPE and DQ are determined so that the effective weak Hamiltonian for quarks give both consistently. The results are compared with current available data. We find that the OPE+DQ superposed transition potential reproduce the currently available experimental data fairly well.

In sec. 2, we present the two-body weak transition potentials for $\Lambda N \rightarrow NN$ in DQ and OPE. In sec. 3, the nuclear wave functions are given. In sec. 4, the results of our calculation are presented and are compared with experiment. Sec. 5 is devoted to conclusions.

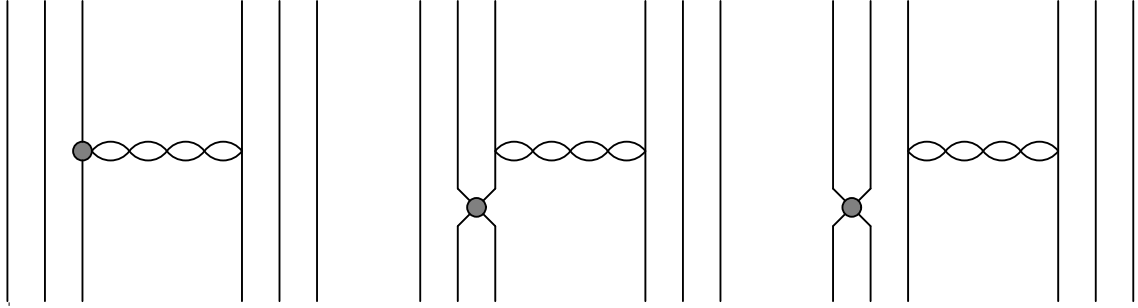


Figure 1: The quark diagrams for the $\Lambda N \rightarrow NN$ transition. \bullet denotes a weak 4-quark vertex.

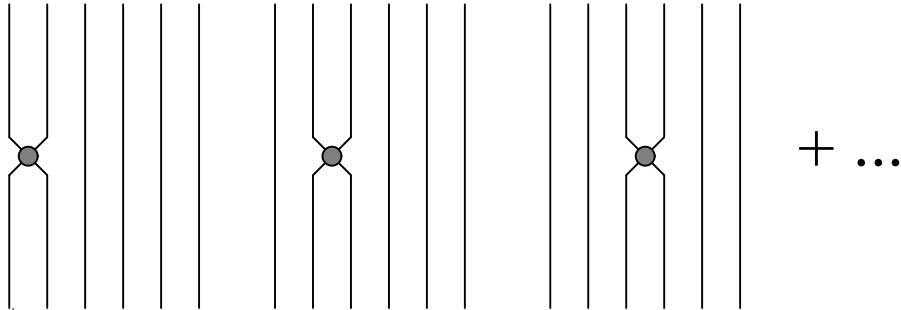


Figure 2: The quark diagrams for the $\Lambda N \rightarrow NN$ transition. \bullet denotes a weak 4-quark vertex.

2. Weak transition potential for $\Lambda N \rightarrow NN$

Considering that a baryon has three constituent quarks, $\Lambda N \rightarrow NN$ process can be described by the diagram, such as those shown in Fig. 1 and Fig. 2. In the diagrams shown in Fig. 1, the strangeness changing weak interaction and an emission of a constituent quark anti-quark pair take place in the Λ hyperon, and the pair is absorbed by a constituent quark in the nucleon. The diagrams in Fig. 2 show the weak interaction of two constituent quarks in a totally anti-symmetric six constituent quark state. The first picture might be well represented by the diagram in Fig. 3, where the baryon is a Dirac particle and couples to, for example, a pion by a phenomenological Yukawa type vertex. This is the one called the meson exchange mechanism and has been studied well[3,4,5,6,7,8]. Though this picture is very natural, one sees that this picture cannot be valid in the region where the two baryons overlap with each other. In such a region, the diagrams in Fig. 2, namely the direct quark process, might cause the $\Lambda N \rightarrow NN$ transition.

Recently, Inoue, Takeuchi and Oka pointed out the importance of the direct quark (DQ) processes and derived the DQ transition potential for the $\Lambda N \rightarrow NN$ systems[11,12,13,14]. There we employed the nonrelativistic constituent quark model for the baryons and the two baryon states are constructed according to the quark cluster model, which takes the full quark antisymmetrization

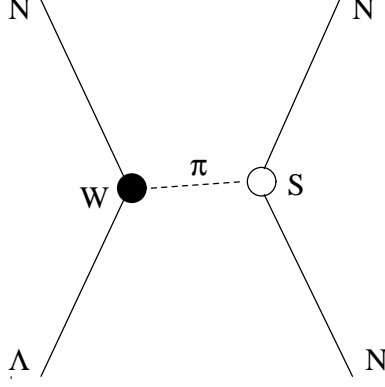


Figure 3: One pion exchange diagram.

into account,

$$|B_1 B_2(k, L, S, J)\rangle = \mathcal{A} |\phi_1 \phi_2 \chi(k)(L, S, J)\rangle \quad (1)$$

where ϕ_1 and ϕ_2 denote the internal wave functions of the baryon B_1 and B_2 and $\chi(k)$ describes the radial part of the relative motion of the baryons with k relative momentum. \mathcal{A} is the quark antisymmetrization operator.

The weak interaction is represented by the effective Hamiltonian,

$$H_{eff}^{\Delta S=1} = -\frac{G_f}{\sqrt{2}} \sum_{r=1, r \neq 4}^6 K_r O_r, \quad (2)$$

where

K_1	K_2	K_3	K_5	K_6
-0.284	0.009	0.026	0.004	-0.021

and

$$O_1 = (\bar{d}_\alpha s_\alpha)_{V-A} (\bar{u}_\beta u_\beta)_{V-A} - (\bar{u}_\alpha s_\alpha)_{V-A} (\bar{d}_\beta u_\beta)_{V-A} \quad (3)$$

$$O_2 = (\bar{d}_\alpha s_\alpha)_{V-A} (\bar{u}_\beta u_\beta)_{V-A} + (\bar{u}_\alpha s_\alpha)_{V-A} (\bar{d}_\beta u_\beta)_{V-A} \\ + 2(\bar{d}_\alpha s_\alpha)_{V-A} (\bar{d}_\beta d_\beta)_{V-A} + 2(\bar{d}_\alpha s_\alpha)_{V-A} (\bar{s}_\beta s_\beta)_{V-A} \quad (4)$$

$$O_3 = 2(\bar{d}_\alpha s_\alpha)_{V-A} (\bar{u}_\beta u_\beta)_{V-A} + 2(\bar{u}_\alpha s_\alpha)_{V-A} (\bar{d}_\beta u_\beta)_{V-A} \\ - (\bar{d}_\alpha s_\alpha)_{V-A} (\bar{d}_\beta d_\beta)_{V-A} - (\bar{d}_\alpha s_\alpha)_{V-A} (\bar{s}_\beta s_\beta)_{V-A} \quad (5)$$

$$O_5 = (\bar{d}_\alpha s_\alpha)_{V-A} (\bar{u}_\beta u_\beta + \bar{d}_\beta d_\beta + \bar{s}_\beta s_\beta)_{V+A} \quad (6)$$

$$O_6 = (\bar{d}_\alpha s_\beta)_{V-A} (\bar{u}_\beta u_\alpha + \bar{d}_\beta d_\alpha + \bar{s}_\beta s_\alpha)_{V+A}. \quad (7)$$

This is derived from the W exchange diagrams in the standard theory, by taking perturbative corrections due to the strong interaction[17]. We evaluated the two-baryon matrix elements of the effective weak Hamiltonian $H_{eff}^{\Delta S=1}$, using the six-quark wave functions given in eq.(1),

$$V(k, k')_{L_i, S_i, J} = \langle NN(k', L_f, S_f, J) | H_{eff}^{\Delta S=1} | \Lambda N(k, L_i, S_i, J) \rangle . \quad (8)$$

Here, k, L, S, J stand for the relative momentum of two baryons, the orbital angular momentum, the spin, and the total angular momentum of the initial and the final states, respectively. The obtained two-body transition amplitudes are regarded as the transition potential in the momentum representation for each channel specified by L, S and J . Fig. 4 shows various diagrams contributing to the transition potential, where the dots represent the weak four quark vertices. The explicit forms of the transition potential is given in ref.[14].

In the present study, we calculate the decays of the s-shell hypernuclei from its ground states. If we employ the simplest shell model wave functions for the hypernuclei, we only need the $L_i = 0$ transition potentials. The relevant transition channels are given in Table 1. The direct quark induced transition potential depends on two quark model parameters that are the constituent quark mass, m , and the Gaussian parameter, b . We use $m = 313 = M_N/3$ MeV and $b = 0.5$ fm in the present calculation.

As for the meson exchange weak transition, we here consider only the one-pion exchange (OPE) process, and will discuss other contributions later. The pion exchange transition potential is obtained by evaluating the diagram like Fig. 3. We here employ the following strong and weak pion vertices,

$$H_{NN\pi}^s = ig_s \bar{\psi}_p \gamma_5 \pi^0 \psi_p - ig_s \bar{\psi}_n \gamma_5 \pi^0 \psi_n + i\sqrt{2}g_s \bar{\psi}_p \gamma_5 \pi^+ \psi_n + i\sqrt{2}g_s \bar{\psi}_n \gamma_5 \pi^- \psi_p \quad (9)$$

$$H_{\Lambda N\pi}^w = ig_w \bar{\psi}_n (1 + \lambda \gamma_5) \pi^0 \psi_\Lambda - i\sqrt{2}g_w \bar{\psi}_p (1 + \lambda \gamma_5) \pi^+ \psi_\Lambda \quad (10)$$

where the strong coupling constant g_s is chosen as the standard value of the πNN coupling: $g_s = -13.26$. The weak coupling constants g_w and λ are determined so as to reproduce the $\Lambda \rightarrow N\pi$ decay amplitudes:

$$g_w = -2.3 \times 10^{-7} \quad (11)$$

$$\lambda = -6.9 . \quad (12)$$

The relative sign of g_s and g_w is important when we consider the interference of OPE and DQ contributions. Namely, g_w must be chosen consistently with our weak Hamiltonian for quarks

and the baryon wave functions. In order to check the consistency, we use the soft pion theorem. Consider the parity-violating part of the $\Lambda \rightarrow n\pi^0$ decay matrix element in the soft pion limit,

$$\lim_{q \rightarrow 0} \langle n\pi^0(q) | H_{eff}(PV) | \Lambda \rangle = -\frac{i}{f_\pi} \langle n | [Q_5^3, H_{eff}(PV)] | \Lambda \rangle . \quad (13)$$

The soft-pion limit is taken by assuming

$$\langle \pi^0(q) | A_\mu^a(x) | 0 \rangle = -if_\pi q_\mu \exp(iq \cdot x) . \quad (14)$$

Note that the Goldberger Treiman relation

$$f_\pi = \frac{Mg_A}{(-g_s)} \quad (15)$$

is satisfied, where g_s is the strong πNN coupling constant defined in eq.(9). Because $H_{eff}(\Delta S = 1)$ consists only of the left-handed currents and the flavor singlet right-handed currents, we have

$$[Q_5^3, H_{eff}(PV)] = [Q_R^3 - Q_L^3, H_{eff}(PV)] \quad (16)$$

$$= -[Q_R^3 + Q_L^3, H_{eff}(PC)] = -[I_3, H_{eff}(PC)] \quad (17)$$

Thus we obtain

$$\lim_{q \rightarrow 0} \langle n\pi^0(q) | H_{eff}(PV) | \Lambda \rangle = \frac{ig_s}{2Mg_A} \langle n | H_{eff}(PC) | \Lambda \rangle \quad (18)$$

Comparing this with the effective hamiltonian eq.(10), the weak πNN coupling constant is given by

$$g_w = \frac{g_s}{2Mg_A} \langle n | H_{eff}(PC) | \Lambda \rangle < 0 \quad (19)$$

after evaluating the matrix element in the right hand side, which is positive with our definition of the Hamiltonian $H_{eff}^{\Delta S=1}$ and the quark model wave function.

In Table 1, we summarize the radial part of the OPE transition potential for the nine possible channels which appear in the calculation for the s-shell hypernuclei. The function in the table are defined by

$$f(r) = \frac{g_w g_s}{4\pi} \frac{\tilde{m}_\pi}{2M} \tilde{m}_\pi \frac{e^{-\tilde{m}_\pi r}}{\tilde{m}_\pi r} \quad (20)$$

$$V(r) = 1 + \frac{1}{\tilde{m}_\pi r} \quad (21)$$

$$T(r) = \frac{1}{3} + \frac{1}{\tilde{m}_\pi r} + \frac{1}{\tilde{m}_\pi^2 r^2} \quad (22)$$

Table 1: One pion exchange induced transition potential

		spin-orbital	I_{NN}	Potential
a_p	$p\Lambda \rightarrow pn$	$^1S_0 \rightarrow ^1S_0$	1	$-\frac{1}{\sqrt{2}}\lambda\frac{\tilde{m}_\pi}{2M}f(r)$
b_p		$\rightarrow ^3P_0$	1	$i\frac{1}{\sqrt{2}}V(r)f(r)$
c_p		$^3S_1 \rightarrow ^3S_1$	0	$-\frac{1}{\sqrt{2}}\lambda\frac{\tilde{m}_\pi}{2M}f(r)$
d_p		$\rightarrow ^3D_1$	0	$-6\lambda\frac{\tilde{m}_\pi}{2M}T(r)f(r)$
e_p		$\rightarrow ^1P_1$	0	$i\sqrt{\frac{3}{2}}V(r)f(r)$
f_p		$\rightarrow ^3P_1$	1	$-i\sqrt{\frac{1}{3}}V(r)f(r)$
a_n	$n\Lambda \rightarrow nn$	$^1S_0 \rightarrow ^1S_0$	1	$-\lambda\frac{\tilde{m}_\pi}{2M}f(r)$
b_n		$\rightarrow ^3P_0$	1	$iV(r)f(r)$
f_n		$^3S_1 \rightarrow ^3P_1$	1	$-i\sqrt{\frac{2}{3}}V(r)f(r)$

when the form factor is not taken account. Here \bar{M} is the average mass of the baryons and $\tilde{m}_\pi = \sqrt{m_\pi^2 - q_0^2}$ is an effective pion mass introduced in order to take care of the finite energy transfer. The radial functions are modified when the form factor with a cutoff Λ_π is introduced, so that

$$f(r) \rightarrow f(r) - \left(\frac{\Lambda_\pi}{\tilde{m}_\pi}\right)^3 f(\Lambda_\pi r) \quad (23)$$

$$f(r)V(r) \rightarrow f(r)V(r) - \left(\frac{\Lambda_\pi}{\tilde{m}_\pi}\right)^3 f(\Lambda_\pi r)V(\Lambda_\pi r) \quad (24)$$

$$f(r)T(r) \rightarrow f(r)T(r) - \left(\frac{\Lambda_\pi}{\tilde{m}_\pi}\right)^3 f(\Lambda_\pi r)T(\Lambda_\pi r). \quad (25)$$

In the present calculation, we choose $\Lambda_\pi^2 = 20\tilde{m}_\pi^2$, according to ref.[4].

We regard DQ and OPE as independent of each other. Fig. 4 shows the various diagrams which contribute to the DQ transition potential. Among them, the diagrams (b) - (g) contain the quark exchange between the two baryons, and therefore the range of the DQ potential is determined by the size of the quark wave function of the baryon. Thus, their contributions are independent from the one-pion exchange, as the strong repulsion due to the quark-exchange is independent from the one-pion exchange potential in the nuclear force.

As the diagram (a), on the other hand, gives a long-range contribution, it may cause a double counting problem. This is the process in which Λ decays into n with another nucleon as a spectator.

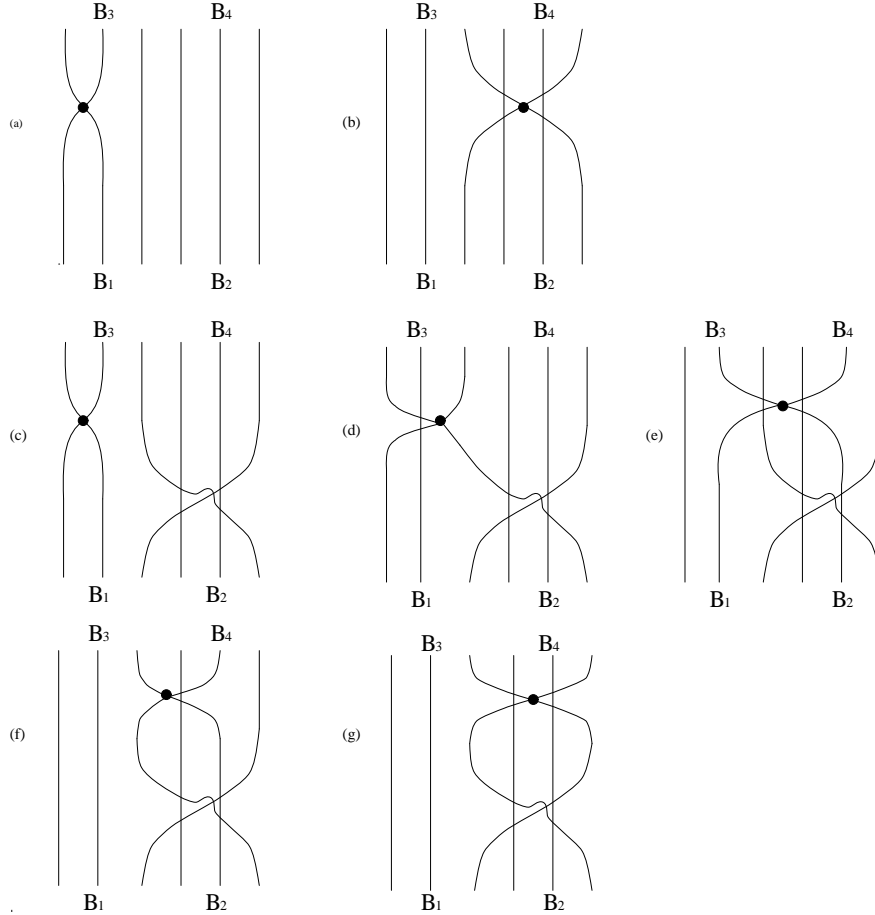


Figure 4: The direct quark transitions. \bullet denotes a weak 4-quark vertex.

Its matrix element is nonzero only through high momentum components of the two baryon wave functions and therefore comes mainly from the short-range correlation of the baryons. Because the one-pion exchange seems not responsible for the short-range correlation, we also regards the diagram (a) as independent. It should also be noted that the contribution of the diagram (a) is in general small as is expected.

3. Initial and final wave functions

For the s-shell hypernuclei, we employ a shell model wave function for the nucleon core, denoted by cluster, x . It has been pointed out that it is important to solve the Λ single particle state carefully using the realistic Λ -nucleon interaction[27]. We denote the relative motion of the Λ hyperon against the nucleon cluster x by a wave function $\Psi(\mathbf{r}_\Lambda)$ with \mathbf{r}_Λ , relative coordinate. The Hamiltonian H of the Λ - x system is given by the sum of the kinetic energy T and a potential energy $V_{\Lambda x}$. The

potential energy $V_{\Lambda x}$ is obtained by folding the potential energy between Λ and the nucleons. In the present study, we construct it by folding the YNG potential with $(0s)^x$ where x stands for the number of nucleon in the cluster x . The YNG potential is a three-range Gaussian potential which reproduces the G-matrix for the Nijmegen ΛN potential model D[24]. The Fermi momentum k_f is fixed 0.9 fm^{-1} for light hypernuclei.

The Schrödinger equation is solved variationally using the local Gaussian basis functions. We expand the wave function for the state which has orbital angular momentum l and the spin S as

$$\Psi(\mathbf{r}_\Lambda) = \sum_d f_{lj}(d) |\Phi(l; d), S; j\rangle . \quad (26)$$

where $j = l + S$. The spin of hypernuclei, S , is the sum of total angular momentum of the cluster x , \mathbf{J}_x , and the spin of Λ , \mathbf{S}_Λ . In eq.(26), $\Phi(l; d)$ is the basis function given by

$$\Phi(l; d) = \phi_l(r_\Lambda; d) Y_l(\hat{\mathbf{r}}_\Lambda) \quad (27)$$

$$\phi_l(r_\Lambda; d) = 4\pi(\sqrt{\pi}b_{\Lambda x})^{-3/2} \exp\left[-\frac{(r_\Lambda^2 + d^2)}{2b_{\Lambda x}}\right] \mathcal{J}_l\left(\frac{r_\Lambda d}{b_{\Lambda x}^2}\right) \quad (28)$$

$$b_{\Lambda x} = \sqrt{\frac{(M_\Lambda + xM_N)}{xM_\Lambda}} b_N . \quad (29)$$

The parameter d can be considered as a generator coordinate describing the distance between two clusters. The \mathcal{J}_l is the l -th order modified spherical Bessel function. The choice of $b_{\Lambda x}$ as in eq(29) enables us to use the Talmi-Moshinsky transformation coefficients in calculating the two-body matrix elements later. The variational amplitudes f_{lj} satisfy the generator coordinate method equation

$$\sum_{d_2} [H_{lj}(d_1, d_2) - EN_{lj}(d_1, d_2)] f_{lj}(d_2) = 0 \quad (30)$$

where the energy and the normalization kernels are given by

$$H_{lj}(d_1, d_2) = \langle \Phi(l; d_1), S; j | H | \Phi(l; d_2), S; j \rangle \quad (31)$$

$$N_{lj}(d_1, d_2) = \langle \Phi(l; d_1), S; j | 1 | \Phi(l; d_2), S; j \rangle . \quad (32)$$

For the hypernucleus ${}^5_\Lambda\text{He}$, we take the Gaussian parameter b_N for $0s$ as 1.358 fm [25,26]. We present the folding potential for even l state in Fig 5. With the following seven values for d ,

$$d = 0.0, 1.0, 2.5, 4.0, 5.5, 7.0 \text{ and } 8.0 \text{ fm}. \quad (33)$$

we obtain the ground state energy $E = -3.08 \text{ MeV}$ and corresponding variational amplitudes.

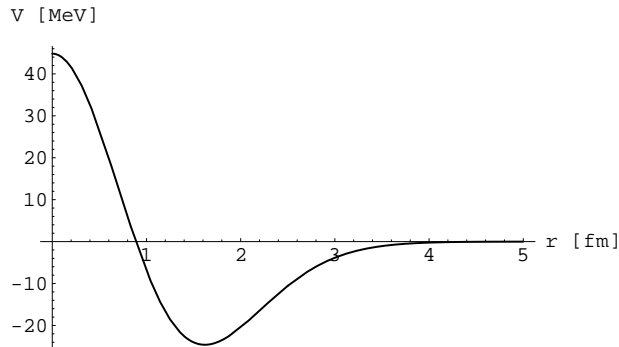


Figure 5: Folded potential for ${}^5_{\Lambda}\text{He}$ for even l state.

Fig 6 shows the obtained wave function $\Psi(\mathbf{r})$. This wave function is considerably different from the one which is obtained with the one range Gaussian (ORG) potential. As shown in Fig 5, the potential $V_{\Lambda x}$ is repulsive at the short distance, reflecting the presence of a repulsive soft core in the YNG interaction. Therefore the obtained wave function is pushed out. This feature gives rise to a sizable difference in the r.m.s. distance between α and Λ , 3.06 fm for YNG while 2.69 fm for ORG[25,26]. Motoba *et al.* applied this wave function to the pionic decay of the s-shell hypernuclei and found that the YNG wave function gives a better agreement to experiment than the ORG one[27,28].

The wave function $\Psi(\mathbf{r}_{\Lambda})$ for ${}^4_{\Lambda}\text{He}$ (or ${}^4_{\Lambda}\text{H}$) is calculated in the same way. In the 4-body case, the Gaussian parameter b_N is taken as 1.65 fm[25,26].

The ΛN wave function, $\Psi_{\Lambda N}$, is given by the product of the above wave function, $\Psi(\mathbf{r}_{\Lambda})$, and nucleon wave function, $\Psi_N(\mathbf{r}_N)$, which is assumed as a Gaussian,

$$\Psi_{\Lambda N}(\mathbf{r}_{\Lambda}, \mathbf{r}_N) = \Psi(\mathbf{r}_{\Lambda}) \times \Psi_N(\mathbf{r}_N) . \quad (34)$$

We perform the Talmi-Moshinsky transform for the two-baryon ΛN wave function $\Psi_{\Lambda N}$ in order to separate the relative motion and the center of mass motion. Defining $\mathbf{r} = \mathbf{r}_{\Lambda} - \mathbf{r}_N$ and the two-baryon center-of mass coordinate \mathbf{R} , the product wave function can be expanded as

$$\Psi_{\Lambda N}(\mathbf{r}, \mathbf{R}) = \sum_{nN} W_{nN} u_{n0}(r, b_r) Y_{00}(\hat{\mathbf{r}}) u_{N0}(R, b_R) Y_{00}(\hat{\mathbf{R}}) , \quad (35)$$

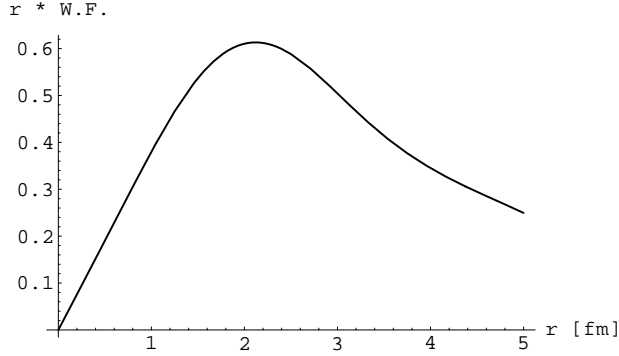


Figure 6: Wave function for Λ - α system.

where u_{n0} is the harmonic oscillator eigenfunctions for $(n, l = 0)$, and

$$b_r = \sqrt{\frac{M_\Lambda + M_N}{M_\Lambda}} b_N \quad (36)$$

$$b_R = \sqrt{\frac{M_\Lambda + x M_N}{(x-1)(M_\Lambda + M_N)}} b_N . \quad (37)$$

The b parameters, A=4 are $b_r = 2.24$ fm, $b_R = 1.61$ fm, and for A=5 are $b_r = 1.84$ fm, $b_R = 1.21$ fm, respectively.

We consider the short-range correlation between Λ and N . In evaluating the OPE transition amplitude, we use the short range correlation obtained for the Nijmegen Λ - N potential model D[25,26]. The Nijmegen model D, however, has a hard repulsive core at short distance, which seems inconsistent with the constituent quark picture. Therefore, in evaluating the matrix element of the DQ transition potential, we use the following form of the short range correlation,

$$u_{n0}(r, b_r) \rightarrow \frac{1}{N} u_{n0}(r, b_r) \left(1 - C_i \exp\left[-\frac{r^2}{r_i^2}\right] \right) . \quad (38)$$

Here, C_i and r_i are parameters, and N is a normalization factor.

As wave function of the outgoing two nucleons in the final state, we employ the scattering state obtained in the Nijmegen model D[25,26]. On the other hand, we use the plane wave with the following form of the short range correlation in evaluating the DQ contribution because of the

same reason stated above.

$$j_l(kr) \rightarrow j_l(kr) \left(1 - C_f \exp\left[-\frac{r^2}{r_f^2}\right] \right) \quad (39)$$

We evaluate the DQ matrix elements for several choices of the parameters for the short-range correlation, while we assume $C_f = C_i$ and $r_f = r_i$ for simplicity.

4. Results and Discussion

In this section, we present our results and compare them with experiment. The experimental data are taken from ref[29,30,31,32,33,34,35,36].

The nonmesonic decay rate of the hypernucleus is given by

$$\Gamma = \sum_f \delta(E.C.) |\langle \Psi_f | V^{weak} | \Psi_i \rangle|^2 \quad (40)$$

where $\delta(E.C.)$ stands for the delta function for the energy conservation. For the final state, we observe only the two nucleons outgoing in the decay. Denoting the momenta of the nucleons as k_1 and k_2 , we find

$$\Gamma = \int \frac{dk_1}{(2\pi)^3} \frac{dk_2}{(2\pi)^3} 2\pi \delta(E.C.) \sum_{res} |\langle k_1, k_2, \Psi_{res} | V^{weak} | \Psi_i \rangle|^2 \quad (41)$$

and

$$\delta(E.C) = \delta \left(M_{res} + 2M_N + \frac{k_1^2}{2M_N} + \frac{k_2^2}{2M_N} - M_{res} - M_\Lambda - E_\Lambda - M_N - E_N \right). \quad (42)$$

Here V^{weak} is a two-body transition potential, and Ψ_i can be expressed as

$$\Psi_i = \sum_{ch} \Psi_{res} \times \Psi_{\Lambda N(ch)} \times (\text{cfp for initial state for channel } ch) \quad (43)$$

for which the spin is implicit. It is easy to obtain the (cfp) for the initial state in the present $(0s)^x + \Lambda$ configuration, resulting a factor for the number of pairs and their spin average factor for each channel, labeled by $a-f$ in Table 1, of the ΛN states. It should be noted that these channels do not interfere with others. Thus we obtain $\Gamma = \sum_{ch} \Gamma_{ch}$, and the decay rate for each channel is given by

$$\Gamma_{ch} = [\# \text{ of } \Lambda N \text{ pairs}] \times [\text{spin average factor}] \times \quad (44)$$

$$\int \frac{dk_1}{(2\pi)^3} \frac{dk_2}{(2\pi)^3} 2\pi \delta(E.C.) |\langle k_1, k_2 | V_{ch}^{weak} | \Lambda N \rangle|^2. \quad (45)$$

4.1. ${}^5_{\Lambda}\text{He}$

In ${}^5_{\Lambda}\text{He}$, there are two Λp bonds and two Λn bonds. The Λp or Λn system takes both spin $S=0$ and spin $S=1$ state. Thus the spin average factor becomes $1/4$ ($3/4$) for $S = 0$ ($S = 1$) channel. The total nonmesonic decay rate of ${}^5_{\Lambda}\text{He}$ is given by

$$\Gamma_{nm}({}^5_{\Lambda}\text{He}) = \Gamma_a^p + \Gamma_b^p + \Gamma_c^p + \Gamma_d^p + \Gamma_e^p + \Gamma_f^p + \Gamma_a^n + \Gamma_b^n + \Gamma_f^n \quad (46)$$

where $\Gamma_a^p \sim \Gamma_f^n$ are the partial decay rates and calculated by

$$\Gamma_{a,b}^p = 2\frac{1}{4} \int \frac{d^3\mathbf{k}}{(2\pi)^3} \int \frac{d^3\mathbf{K}}{(2\pi)^3} (2\pi)\delta(E.C.) \left| \langle NN | V_{a,b}^p | \Lambda N \rangle \right|^2 \quad (47)$$

$$\Gamma_{c,d,e,f}^p = 2\frac{3}{4} \int \frac{d^3\mathbf{k}}{(2\pi)^3} \int \frac{d^3\mathbf{K}}{(2\pi)^3} (2\pi)\delta(E.C.) \left| \langle NN | V_{c,d,e,f}^p | \Lambda N \rangle \right|^2 \quad (48)$$

$$\Gamma_{a,b}^n = 2\frac{1}{4} \int \frac{d^3\mathbf{k}}{(2\pi)^3} \int \frac{d^3\mathbf{K}}{(2\pi)^3} (2\pi)\delta(E.C.) \left| \langle NN | V_{a,b}^n | \Lambda N \rangle \right|^2 \quad (49)$$

$$\Gamma_f^n = 2\frac{3}{4} \int \frac{d^3\mathbf{k}}{(2\pi)^3} \int \frac{d^3\mathbf{K}}{(2\pi)^3} (2\pi)\delta(E.C.) \left| \langle NN | V_f^n | \Lambda N \rangle \right|^2 . \quad (50)$$

First we study the OPE mechanism. Table 2 shows the partial decay rates obtained for the one pion exchange potential. All the decay rates are written in the unit of Γ_{Λ} , the free Λ decay rate. We list three sets of results. The values listed under ‘‘OFF’’ are the results when we omit the form factor and the short range correlation into account. The values listed under ‘‘FF’’ are the result when we take only the form factor into account. The values listed under ‘‘FF and SRC’’ are the final result with both the form factor and the short range correlation taken into account. Because $\Delta I = 1/2$ is assumed for the weak $\Lambda N\pi$ vertex, these partial decay rates satisfy the isospin relation $a_n/a_p = b_n/b_p = f_n/f_p = 2$.

In the ‘‘OFF’’ and ‘‘FF’’ cases, the channel d_p is dominant. This comes from the tensor part of the transition potential, which is enhanced due to the large relative momentum in the final state. One can see that the form factor reduces most of the partial decay rates significantly. In the ‘‘FF and SRC’’ case, the channel c_p becomes large and is dominant. This comes also from the tensor part of the transition potential together with the tensor part of the final state interaction. In the OPE mechanism, the channel e_p has also a large rate, while the rates in the channels a and b are very small.

Table 2 shows calculated nonmesonic decay rates of ${}^5_{\Lambda}\text{He}$ in OPE. We list the proton induced decay rate (Γ_p), the neutron induced decay rate (Γ_n), the total decay rate ($\Gamma_{nm} = \Gamma_p + \Gamma_n$), and the n - p ratio ($R_{np} = \Gamma_n/\Gamma_p$). The experimental data are listed in Table 5. One can see that the calculated Γ_p is in good agreement with experiment, while the calculated Γ_n is much smaller than

Table 2: Calculated nonmesonic decay rates of ${}^5_{\Lambda}\text{He}$ in the one pion exchange mechanism (in the unit of Γ_{Λ} , the decay rate of the free Λ).

Ch	OFF	FF	FF and SRC
a_p	0.0004	0.0101	0.0002
b_p	0.0126	0.0060	0.0031
c_p	0.0013	0.0303	0.1022
d_p	0.3918	0.1789	0.0415
e_p	0.1132	0.0544	0.0346
f_p	0.0251	0.0121	0.0093
a_n	0.0009	0.0202	0.0003
b_n	0.0251	0.0121	0.0063
f_n	0.0502	0.0242	0.0186
Γ_p	0.544	0.291	0.191
Γ_n	0.076	0.056	0.025
Γ_{nm}	0.621	0.348	0.216
R_{np}	0.140	0.193	0.130

experiment. The Γ_p is dominated by large contribution of the channels c and d , which vanish in the neutron induced decay. Thus the calculated n - p ratio is much smaller than the experimental one.

We turn to the DQ mechanism. Table 3 shows the partial decay rates when we employ the direct quark induced potential. We list four sets of result which are calculated with different short range correlations, while we assume $r_i = r_f$ and $C_i = C_f = C$ for simplicity. The parameter r_0 is fixed as 0.5 fm, which is equal to the Gaussian parameter b in the quark model. The partial decay rate for channel d_p is zero, because the direct quark potential has no $\Delta L = 2$ part due to the nonrelativistic truncation at the first order in p/m . The total decay rates, Γ_p , Γ_n and Γ_{nm} decrease as the short range correlation strength C_i or C_f increases. This is natural because the short range correlation reduces the inner part of the wave functions where the direct quark mechanism is important.

Compared to the results in Table 2, we find that the overall magnitudes of the decay rates are comparable to OPE. The components, however, are different. For the proton induced decays, OPE is dominated by the $I = 0$ final states, c_p , d_p , and e_p , while the DQ gives a large decay rates to

Table 3: Calculated nonmesonic decay rates of ${}^5_{\Lambda}\text{He}$ in the direct quark mechanism (in the unit of Γ_{Λ} , the decay rate of the free Λ).

Ch	$C = 0$	$C = 0.3$	$C = 0.5$	$C = 0.7$
a_p	0.0130	0.0150	0.0167	0.0185
b_p	0.0127	0.0120	0.0113	0.0105
c_p	0.0968	0.0690	0.0548	0.0440
d_p	0	0	0	0
e_p	0.0056	0.0061	0.0064	0.0067
f_p	0.0345	0.0353	0.0353	0.0352
a_n	0.0727	0.0516	0.0407	0.0322
b_n	0.0059	0.0066	0.0069	0.0073
f_n	0.0622	0.0642	0.0648	0.0650
Γ_p	0.163	0.137	0.125	0.115
Γ_n	0.141	0.122	0.112	0.104
Γ_{nm}	0.304	0.260	0.237	0.219
R_{np}	0.865	0.889	0.903	0.910

the $I = 1$ final states, a_p , b_p , and f_p . The neutron induced decays go only to the $I = 1$ states, a_n , b_n , and f_n , and thus the DQ gives much larger contribution than OPE. It should also be stressed that the $J = 0$ channels play major roles in DQ, while the OPE is dominated by $J = 1$. It is important to note that these general features can be tested in the decays of the s-shell hypernuclei. For instance, we will see that DQ must be dominant in the decay of ${}^4_{\Lambda}\text{H}$ because the $I = 0$ final states are prohibited there.

Next we investigate the ΔI property of the direct quark mechanism. In the following, we employ $C_i = C_f = C = 0.5$. Table 4 shows the effects of the $\Delta I = 3/2$ part of the potential. The values listed under ‘‘DQ full’’ are the results when we employ the full direct quark induced potential. While the values listed under ‘‘ $\Delta I = 1/2$ only’’ are the results when we omit the $\Delta I = 3/2$ part. One sees that the channels a and b , which are $J = 0$ transitions, get significant contribution from the $\Delta I = 3/2$ part. This indicates that $\Delta I = 1/2$ rule is broken significantly in the non-mesonic decays of light hypernuclei.

The large $\Delta I = 3/2$ transition is very interesting. It is, in fact, expected naturally in the

Table 4: Calculated nonmesonic decay rates of ${}^5_{\Lambda}\text{He}$ in the direct quark mechanism ($C_i = C_f = C = 0.5$). The partial rates, c_p , d_p and e_p do not have $\Delta I = 3/2$ contribution because the final state has $I = 0$.

Ch	$\Delta I = 1/2$ only	DQ full
a_p	0.0118	0.0167
b_p	0.0001	0.0113
f_p	0.0334	0.0353
a_n	0.0237	0.0407
b_n	0.0003	0.0069
f_n	0.0668	0.0648

standard theory of the weak interaction. But one may wonder whether the present quark model with Hamiltonian $H_{eff}^{\Delta S=1}$ is capable to reproduce the $\Delta I = 1/2$ dominance of the free hyperon decay. In order to check it, we study the free Λ decay with this effective Hamiltonian[37]. We find the dominance of quark diagrams with internal weak vertex in which $\Delta I = 3/2$ amplitudes vanish, according to the Pati-Woo theorem which is resulted from the color symmetry of the ground state baryons[38]. Therefore, the dominant decay of the hyperons go through the $\Delta I = 1/2$ part of the Hamiltonian. It is extremely interesting to confirm the strong $\Delta I = 3/2$ weak transition.

The calculated Γ_p , Γ_n , Γ_{nm} , and R_{np} in DQ are shown in Table 3. The proton induced decay rate Γ_p in DQ is smaller than that of OPE. On the other hand, the neutron induced decay rate Γ_n in DQ is much larger than that of the OPE. This is due to large contribution of channel a_n and f_n . The total nonmesonic decay rate in DQ is roughly equal, while the n - p ratio in DQ is much larger than that of OPE and is about 0.9, which is closer to the experimental data.

As was argued in the section 2, the final results are given by the superposition of the OPE and DQ processes. Table 5 summarizes the results given by the sum of the two transition potentials. We find that the neutron induced decay rate, Γ_n , is significantly enhanced from OPE and becomes consistent with experimental data. On the other hand, the combined result overestimates the proton induced decay rate, Γ_p . Thus the total decay rate, Γ_{nm} , is slightly overestimated. The n - p ratio, R_{np} , is predicted in between the values for OPE and DQ, while the experimental data suggest larger values.

Table 5: Calculated nonmesonic decay rates of ${}^5_{\Lambda}\text{He}$ (in the unit of Γ_{Λ}).

Ch	OPE only	DQ only	OPE + DQ	EXP[29]	EXP[30]
a_p	0.0002	0.0167	0.0188		
b_p	0.0031	0.0113	0.0026		
c_p	0.1022	0.0548	0.2612		
d_p	0.0415	0	0.0415		
e_p	0.0346	0.0064	0.0207		
f_p	0.0093	0.0353	0.0763		
a_n	0.0003	0.0407	0.0356		
b_n	0.0063	0.0069	0.0264		
f_n	0.0185	0.0648	0.1437		
Γ_p	0.191	0.125	0.421	0.21 ± 0.07	0.17 ± 0.04
Γ_n	0.025	0.112	0.206	0.20 ± 0.11	0.33 ± 0.04
Γ_{nm}	0.216	0.237	0.627	0.41 ± 0.14	0.50 ± 0.07
R_{np}	0.132	0.903	0.489	0.93 ± 0.55	1.97 ± 0.67

4.2. ${}^4_{\Lambda}\text{He}$

In the ${}^4_{\Lambda}\text{He}$, there are two Λp bonds and one Λn bond. The Λn pair is in the spin $S=0$ state so that the spin of ${}^4_{\Lambda}\text{He}$ is equal to zero. Thus there is no contribution from the channel f_n . The the partial decay rates of are given by

$$\Gamma_{a,b}^p = 2\frac{1}{4}\int\frac{d^3\mathbf{k}}{(2\pi)^3}\int\frac{d^3\mathbf{K}}{(2\pi)^3}(2\pi)\delta(E.C.)\left|\langle NN|V_{a,b}^p|\Lambda N\rangle\right|^2 \quad (51)$$

$$\Gamma_{c,d,e,f}^p = 2\frac{3}{4}\int\frac{d^3\mathbf{k}}{(2\pi)^3}\int\frac{d^3\mathbf{K}}{(2\pi)^3}(2\pi)\delta(E.C.)\left|\langle NN|V_{c,d,e,f}^p|\Lambda N\rangle\right|^2 \quad (52)$$

$$\Gamma_{a,b}^n = \int\frac{d^3\mathbf{k}}{(2\pi)^3}\int\frac{d^3\mathbf{K}}{(2\pi)^3}(2\pi)\delta(E.C.)\left|\langle NN|V_{a,b}^n|\Lambda N\rangle\right|^2. \quad (53)$$

Table 6 shows our results and the experimental data. The results of OPE are qualitatively the same to ${}^5_{\Lambda}\text{He}$, but are reduced to 80 % or less. On the other hand, the results of DQ have qualitative differences. The rates in the channels c_p and a_n are very small, which are large in the ${}^5_{\Lambda}\text{He}$ case. This indicates that the DQ contribution is sensitive to the wave function of the initial ΛN system. Again the full calculation of OPE+DQ provides a good agreement to the experimental data except that Γ_p is again slightly overestimated. In our result, Γ_n is dominated by the channel b .

Table 6: Calculated nonmesonic decay rates of ${}^4_{\Lambda}\text{He}$ (in the unit of Γ_{Λ}).

Ch	OPE only	DQ only	OPE+DQ	EXP[35]
a_p	0.0001	0.0183	0.0214	
b_p	0.0021	0.0087	0.0023	
c_p	0.0818	0.0004	0.0884	
d_p	0.0321	0	0.0321	
e_p	0.0224	0.0048	0.0140	
f_p	0.0065	0.0275	0.0567	
a_n	0.0005	0.0013	0.0004	
b_n	0.0083	0.0108	0.0380	
f_n	0	0	0	
Γ_p	0.145	0.060	0.214	0.15 ± 0.02
Γ_n	0.009	0.012	0.038	0.04 ± 0.02
Γ_{nm}	0.154	0.072	0.253	0.19 ± 0.04
R_{np}	0.061	0.202	0.178	0.27 ± 0.14

4.3. ${}^4_{\Lambda}\text{H}$

In ${}^4_{\Lambda}\text{H}$, there are one Λp bond and two Λn bonds. The Λp pair is in the spin $S=0$ state so that the spin of ${}^4_{\Lambda}\text{He}$ is equal to zero. Thus there are no contributions from the channels c_p though f_p . The the partial decay rates are given by

$$\Gamma_{a,b}^p = \int \frac{d^3\mathbf{k}}{(2\pi)^3} \int \frac{d^3\mathbf{K}}{(2\pi)^3} (2\pi)\delta(E.C.) \left| \langle NN | V_{a,b}^p | \Lambda N \rangle \right|^2 \quad (54)$$

$$\Gamma_{a,b}^n = 2 \frac{1}{4} \int \frac{d^3\mathbf{k}}{(2\pi)^3} \int \frac{d^3\mathbf{K}}{(2\pi)^3} (2\pi)\delta(E.C.) \left| \langle NN | V_{a,b}^n | \Lambda N \rangle \right|^2 \quad (55)$$

$$\Gamma_f^n = 2 \frac{3}{4} \int \frac{d^3\mathbf{k}}{(2\pi)^3} \int \frac{d^3\mathbf{K}}{(2\pi)^3} (2\pi)\delta(E.C.) \left| \langle NN | V_f^n | \Lambda N \rangle \right|^2 . \quad (56)$$

Table 7 shows our results. In our model, each partial decay rate is the same as that of ${}^4_{\Lambda}\text{He}$ except for the number of bonds and the spin average factor. The effect of the interference of OPE and DQ is large in the channel f_n , which does not appear in the ${}^4_{\Lambda}\text{He}$ decay. At present, the experimental data are very limited. Only the total nonmesonic decay rate is barely known. Our prediction agrees with it. The result also suggests that the neutron induced decay is stronger than the proton. Thus we expect a large n - p ratio for ${}^4_{\Lambda}\text{H}$. We anticipate new good experimental data

Table 7: Calculated nonmesonic decay rates of ${}^4_{\Lambda}\text{H}$ (in the unit of Γ_{Λ}).

Ch	OPE only	DQ only	OPE+DQ	EXP[36]
a_p	0.0003	0.0366	0.0429	
b_p	0.0041	0.0174	0.0046	
a_n	0.0003	0.0006	0.0002	
b_n	0.0041	0.0054	0.0190	
f_n	0.0130	0.0504	0.0107	
Γ_p	0.004	0.054	0.047	
Γ_n	0.017	0.057	0.126	
Γ_{nm}	0.022	0.110	0.174	0.15 ± 0.13
R_{np}	3.952	1.048	2.660	

for the nonmesonic decay of ${}^4_{\Lambda}\text{H}$.

4.4. OTHER CONTRIBUTIONS

So far we considered only the one-pion exchange and the direct quark transitions. Several other possibilities are considered in the following. First we discuss the effect of the heavy meson exchanges. Ramos *et al.* calculated the $\Lambda N \rightarrow NN$ transition in a full one-boson-exchange mechanism[19]. They include the other pseudosclar mesons, η and K , as well as the vector mesons, ρ, ω and K^* . In constructing the transition potential induced by the exchange of the heavy mesons, the Nijmegen or the Jülich strong vertices, $H_{NN\eta}, H_{NNK}, H_{N\rho}, H_{NN\omega}$ and H_{NNK^*} , are employed. On the other hand, the weak vertices, $H_{\Lambda N\eta}, H_{\Lambda NK}, H_{\Lambda N\rho}, H_{\Lambda N\omega}$ and $H_{\Lambda NK^*}$, which cannot be determined from the hyperon-decay experiment, are determined by the $SU(6)$ symmetry and the soft meson theorem for the PV vertices and pole model for the PC vertices[20]. The nonmesonic weak decay of ${}^{13}_{\Lambda}\text{C}$ is studied in the shell model framework. The result shows that the combined $\pi + \rho$ exchange predicts a very similar total decay rate to the OPE one. It is found that the total rate is reduced by more than 40% when K exchange is added. It is also found that K^* exchange compensates the K exchange and that the total rate for the combined $\pi + \rho + K + K^*$ is only 10 % smaller than the OPE only. The contribution of η and ω are very small and tend to cancel each other. Therefore the total rate for the combined $\pi + \rho + K + K^* + \eta + \omega$ is similar to the OPE only. They found that the addition of K exchange reduces the n - p ratio considerably while the addition

of other mesons does not change the result much. The final n - p ratio is smaller than that of OPE, which is much smaller than the experimental data.

Shmatikov studied the 2π exchange contribution. It is indicated that the diagrams with ΣN and NN intermediate states cancel each other and the net effect contributes only to the $J = 0$ amplitudes[21].

Recently, Itonaga *et al.* [26] have studied the $2\pi/\rho$ and $2\pi/\sigma$ exchange weak potentials in which 2π are coupled to ρ and σ , respectively, in the exchange process. The weak vertices $H_{\Lambda N\pi}$ and $H_{\Sigma N\pi}$ are empirically known from the pionic decay of Λ and Σ hyperons and the Lee-Sugawara relations. The strong coupling constants are determined so that the corresponding strong potential versions of the $2\pi/\rho$ and $2\pi/\sigma$ exchanges can simulate the OBE potentials due to ρ and σ exchange, respectively. There is no phase ambiguity between OPE and $2\pi/\rho$ and $2\pi/\sigma$ exchange weak potentials. The $2\pi/\rho$ exchange potential has a tensor part whose sign is opposite to that of the OPE one and thus it tends to weaken the tensor interaction of the latter potential. The $2\pi/\sigma$ exchange is of central type typical from its character. These potentials are applied to the non-mesonic decays of typical hypernuclei ranging from s-shell to medium-heavy systems. The addition of $2\pi/\rho$ exchange decreases the non-mesonic decay rates by 5-10 % with respect to the OPE estimates. The inclusion of both $2\pi/\rho$ and $2\pi/\sigma$ exchanges leads to increase the decay rates of about 5-15 % with respect to the OPE estimate. Calculated non-mesonic decay rates, together with minor contributions from the pionic decay channels, are generally consistent with the lifetimes measured for p- and sd-shell hypernuclei. As for the n/p ratios, the addition of the $2\pi/\rho$ and $2\pi/\sigma$ exchanges does not cause much improvement and the theoretical values are still far from the experimental data.

In all, the meson exchange contributions other than OPE seem to be less important than DQ. Therefore describing the $\Lambda N \rightarrow NN$ transition by the sum of OPE and DQ, seems to be reasonable.

5. Conclusion

It is shown that the one pion exchange mechanism is significant to the nonmesonic decay of light s-shell hypernuclei but is not able to reproduce some of the experimental data. Our result shows that the direct quark processes in $\Lambda N \rightarrow NN$ provides as large contribution as the OPE. We also show that the DQ contribution is qualitatively different from the one pion exchange mechanism. The DQ contribution is dominant in some channels, such as the proton induced $J = 0$ channels, a_p and b_p . It is also shown that the direct quark mechanism causes a large $\Delta I = 3/2$ transition in several channels. Our results are qualitatively consistent with those of Maltman and Shmatikov

[10], although the calculated amplitudes have quantitative differences.

In this paper, we have determined the relative phase of OPE and DQ by using the soft pion relation. Thus we superpose these two mechanisms without ambiguity. We reproduce the present data for ${}^5_{\Lambda}\text{He}$, ${}^4_{\Lambda}\text{He}$ and ${}^4_{\Lambda}\text{H}$ fairly well by superposing OPE and DQ. Some predictions are made for the nonmesonic decays of ${}^4_{\Lambda}\text{H}$, to which experimental data are very limited. It should be stressed that the ratios of the partial rates for various channels are extremely useful in distinguishing different mechanisms of the transition. Further experimental studies are most desirable.

There are a number of remaining problems. In the present analysis, we have not considered so far the second order processes with $\Sigma - N$ intermediate states induced by the pion (meson) and/or quark exchanges. The short range part of weak transition potential for $\Sigma N \rightarrow NN$ was also computed in the same direct quark mechanism[13]. It is found that the mixing of this potential does not change the main feature of present DQ potential, though its contribution depend on the probability of the Σ mixture and is not negligible quantitatively.

For hypernuclei other than the s-shell systems, we need a realistic calculation combined with the nuclear structure analysis. Further study is needed.

References

- [1] J. Cohen, Prog. in Part. and Nucl. Phys. **25**(1990)139
- [2] S. Shinmura Prog. Theor. Phys. **97**(1997)283
- [3] M.M. Block and R.H. Dalitz, Phys. Rev. Lett. **11**(1963)96
- [4] K. Takeuchi, H. Takaki and H. Bando, Prog. Theor. Phys. **73**(1985)841
- [5] B.H.J. Mckellar and B.F. Gibson, Phys. Rev. **C30**(1984)322
- [6] A. Ramos, E. van Meijgaard, C. Bennhold, and B. K. Jennings, Nucl. Phys. **A544**(1992)703
- [7] Y. Abe *et al.*, Prog. Theor. Phys. **64**(1980)1363.
- [8] H. Bando, T. Motoba and J. Zofka, Int. Jour. Mod. Phys. **A5**(1990)4021
- [9] C. Y. Cheung, D. P. Heddle and L. S. Kisslinger, Phys. Rev. **C27**(1983)335
- [10] K. Maltman and M. Shmatikov, Phys. Lett. **B331**(1994)1
- [11] M. Oka, T. Inoue and S. Takeuchi, "Properties & Interactions of Hyperons", ed. by B. F. Gibson, P. D. Barnes and K. Nakai (World Scientific, 1994), P119
- [12] T. Inoue, S. Takeuchi and M. Oka, Nucl. Phys. **A577**(1994)281c
- [13] M. Oka, T. Inoue and S. Takeuchi, Proceedings of the IV International Symposium on Weak and Electromagnetic Interactions in Nuclei, ed. by H. Ejiri, T. Kishimoto and T. Sato (World

- Scientific, 1995), p.540
- [14] T. Inoue, S. Takeuchi and M. Oka, Nucl. Phys. **A597**(1996)563
 - [15] A.I. Vainshtein, V.I. Zakharov and M.A. Shifman, Sov. Phys. JETP, **45**(1977)670
 - [16] F. J. Gilman and M. B. Wise, Phys. Rev. **D20**(1979)2382
 - [17] E.A. Paschos, T. Schneider, and Y.L. Wu, Nucl. Phys. **B332**(1990)285
 - [18] M. Oka and K. Yazaki, Phys. Lett. **B90**(1980)41; Prog. Theor. Phys. **66**(1981)556
 - [19] A. Ramos and C. Bennhold, Nucl. Phys. **A577**(1994)287c,
A. Parreno, A. Ramos, and C.Bennhold, nucl-th/9611030
 - [20] J.F. Dubach, G.B. Feldman, B.R. Holstein and L. de la Torre, Ann. Phys. **249**(1996)146
 - [21] M. Shmatikov, Preprint IAE-5708/2 M. 1994
 - [22] K. Itonaga, T. Ueda and T. Motoba, Nucl. Phys. **A577**(1994)301c
K. Itonaga, T. Ueda and T. Motoba, Nucl. Phys. **A585**(1995)331c
 - [23] M.M Nagels, T.A.Rijken and J.J. deSwart, Phys. Rev. **D12**(1975)744,
Phys. Rev. **D15**(1977)2547, Phys. Rev. **D20**(1979)1633
 - [24] Y.Yamamoto and H.Bandō, Prog. Theor. Phys. **73**(1985)905,
Prog. Theor. Phys. Suppl. **81**(1985)42, Prog. Theor. Phys. **83**(1990)254
 - [25] Y. Yamamoto, T. Motoba, H. Himeno, K. Ikeda and S. Nagata, Prog. Theor. Phys. Suppl. **117**(1994)361
 - [26] T. Motoba and K. Itonaga, Prog. Theor. Phys. Suppl. **117**(1994)477
 - [27] T. Motoba, Nucl. Phys. **A547**(1992)115c
 - [28] I. Kumagai-Fuse *et al.* , Phys. Lett. **B345**(1995)386
 - [29] J.J. Szymanski *et al.* Phys. Rev. **C43**(1991)849
 - [30] H. Noumi, *et al.* Proceedings of the IV International Symposium on Weak and Electromagnetic Interactions in Nuclei, ed. by H. Ejiri, T. Kishimoto and T. Sato (World Scientific, 1995), p.550
 - [31] S. Ajimura *et al.* Phys. Lett. **B282**(1992)293
 - [32] T. Kishimoto, “Properties & Interactions of Hyperons”, ed. by B. F. Gibson, P. D. Barnes and K. Nakai (World Scientific, 1994), p.101
 - [33] R.A. Schumacher, Nucl. Phys. **A547**(1992)143c
 - [34] R.A. Schumacher for the E788 Collaboration “Properties & Interactions of Hyperons”, ed. by B. F. Gibson, P. D. Barnes and K. Nakai (World Scientific, 1994), p.85

- [35] V.J. Zeps and G.B. Franklin for the E788 Collaboration, Proceedings of the 23rd INS International Symposium on Nuclear and Particle Physics with Meson Beams in 1 GeV/c Region, p.227
- [36] H. Ota, *et al.* Proceedings of the IV International Symposium on Weak and Electromagnetic Interactions in Nuclei, ed. by H. Ejiri, T. Kishimoto and T. Sato (World Scientific, 1995), p.532
- [37] T. Inoue, M. Takizawa and M. Oka, to be published.
- [38] J.C. Pati and C.H. Woo, Phys. Rev. **D3**(1971)2920
- K.Miura and T.Minamikawa Prog. Theor. Phys. **38**(1967)954